CHINESE JOURNAL OF PHYSICS VOL. 52, NO. 1-I February 2014

Muon-Electron Hyperfine Coupling Constants of Muoniated Ethyl Radical: a Path Integral Simulation Study with Semiempirical Molecular Orbital Method

Kenta Yamada, Yukio Kawashima, and Masanori Tachikawa

Quantum Chemistry Division, Graduate School of Science,
Graduate School of Nanobioscience, Yokohama City University, Yokohama 236-0027, Japan
(Received December 23, 2012; Revised May 22, 2013)

We have investigated, by *on-the-fly* path integral molecular dynamics (PIMD) simulations, which can take into account the nuclear quantum and thermal effects, the nuclear quantum effect on the muoniated ethyl radical, where one of the hydrogen atoms of the methyl group in the ethyl radical is substituted with a muonium. Muonium consists of a positive muon and an electron, which can be considered as an ultra-light isotope of a hydrogen atom, and we here focused on the muon spin resonance/rotation/relaxation (μSR) and the hyperfine coupling constants (HFCC). Our PIMD simulation with the semiempirical PM6 method has succeeded in treating the nuclear quantum effect, which results mainly in the elongation of the bond length and the characteristic rotation of the CH_2Mu group. Our PIMD simulation provides dramatic improvements in the characteristics of the HFCCs obtained from the conventional PM6 calculation, although the calculated HFCCs are not in qualitative agreement with the corresponding experimental ones because of the limitation of the semiempirical PM6 method for systems with an unpaired electron.

DOI: 10.6122/CJP.52.126 PACS numbers: 31.15.xk, 31.30.Gs, 36.10.Ee

I. INTRODUCTION

A positive muon (μ^+) is the antiparticle of a negative muon (μ^-), which is one of the three known charged leptons. The phrase "muon chemistry" was advocated and this chemistry has been vigorously studied for about three decades [1]. For example, using μ^- for catalysis in nuclear-fusion reactions of H isotopes has been performed [2]. The characteristic feature of μ^+ is its light mass; μ^+ has about 1/9 the mass of the proton (H^+). It captures an electron to form one of the exotic atoms, i.e., muonium (Mu$\equiv \mu^+e^-$), which can be regarded as an ultra-light isotope of an H atom. This indicates that μ^+ is allowed to be treated as a nucleus. Recently, the muoniated radical Br-Mu-Br, formed by Mu addition to Br_2, was claimed to be observed [3]; it has been also discussed in some theoretical studies [4]. Another feature of μ^+ is its magnetic moment; μ^+ has a magnetic moment 3.18 times larger than that of H^+. μ^+ introduced into free radicals can sensitively probe its local environment either directly or through picking-up a electron. The muon spin resonance/rotation/relaxation (μSR), based on the aforementioned features, has been carried out to investigate the electron distributions and geometric structure of free radicals in many experimental studies [1, 5].

In μSR and electron paramagnetic resonance (EPR), a hyperfine coupling constant (HFCC) is an index representing the magnitude of the magnetic interaction between the electronic and nuclear spins. It is well known that the HFCC of a nucleus is proportional

to the spin density at this nucleus, and a large HFCC corresponds to a strong interaction between electron(s) at the nucleus and unpaired electron(s) on another nucleus. The HFCC can be decomposed into an isotropic component (Fermi contact term) and an anisotropic component. The former provides information on the spin density at nuclei of various free radicals, and the latter on the asymmetry of this density.

Theoretical methods have been developed to accurately predict the HFCC [6]. This is because isotropic HFCC is sensitive particularly to both the quality of the one-particle basis functions and the level of the electronic structure theory. In recent years, using the density functional theory (DFT) methods, muoniated as well as hydrogenated free radicals are widely studied to interpret and rationalize experimental results [7]. However, conventional DFT methods, which treat nuclei as point charges, cannot describe the nuclear quantum effect, though it is well known that the quantum behavior of a proton plays a critical role in a system including the H atom [8]. Because of the larger quantum effect of the muon arising from its smaller mass, it is indispensable to use methods that can consider this effect to reveal the nature of a muoniated system.

We have shown that in various molecular systems the quantum effect of a proton makes the difference between the *equilibrium* structure by conventional methods and the *average* structure from the path integral molecular dynamics approach with *ab initio* theory (*ab initio* PIMD approach) [9]. This approach introduces nuclear quantum and thermal effects into conventional molecular orbital (MO) and DFT calculations under the Born-Oppenheimer approximation. To our best knowledge, the present paper is the first application of the PIMD approach to muoniated ethyl radical ($C_\beta H_2$Mu-$C_\alpha H_2$), which is one of the simplest carbon-centered free radicals. Accordingly, first we determine suitable conditions for our PIMD simulations to represent the behavior of the "cloud" of μ^+ in our Results and Discussion section, preceded by the computational details in the following section. Then we start our discussion of the molecular structure and HFCCs in muoniated ethyl radical. Finally, our concluding remarks are presented.

II. COMPUTATIONAL DETAILS

The equilibrium (EQ) structure of muoniated ethyl radical was optimized by the conventional PM6 method [10], one of the semiempirical methods, with the MOPAC 2012 package [11]. Clearly, the EQ structure of muoniated ethyl radical is equal to that of the (hydrogenated) ethyl radical, since the mass of the nucleus does not affect the electronic structure within the conventional approach. Fig. 1 gives a schematic structure of the ethyl radical, constituted of methyl and methylene groups, where the H_1 atom is replaced by a Mu atom in muoniated ethyl radical. To explore the methyl-group rotation and methylene-group rocking motion, two fictitious positions of X and X′ were defined. For this purpose, $\mathbf{R}_\mathrm{A}$ is used to express the coordinate of the A atom and $\mathbf{R}_\mathrm{AB}$ denotes $\mathbf{R}_\mathrm{B} - \mathbf{R}_\mathrm{A}$. At the beginning, X′, represented as the green ball in Fig. 1, was placed on the bisector of

$\angle$H$_4$-C$_\alpha$-H$_5$ ($\theta_{\mathrm{H_4C_\alpha H_5}}$). Thus X$'$ on the plane of the methylene group was defined as

$$\mathbf{R}_{\mathrm{C_\alpha X'}} = \frac{1}{\sqrt{2+2\cos\theta_{\mathrm{H_4C_\alpha H_5}}}}\left(\frac{\mathbf{R}_{\mathrm{C_\alpha H_4}}}{|\mathbf{R}_{\mathrm{C_\alpha H_4}}|}+\frac{\mathbf{R}_{\mathrm{C_\alpha H_5}}}{|\mathbf{R}_{\mathrm{C_\alpha H_5}}|}\right). \tag{1}$$

Meanwhile, for the dihedral angle $\angle$Mu-C$_\beta$-C$_\alpha$-X indicating the angle between the planes of the {Mu, C$_\beta$, C$_\alpha$} atoms and {C$_\beta$, C$_\alpha$, X} atoms, X shown as the purple ball in Fig. 1 was defined through a temporary position vector $\tilde{\mathbf{R}}_{\mathrm{C_\alpha X}}$:

$$\mathbf{R}_{\mathrm{C_\alpha X}} = \begin{cases} \tilde{\mathbf{R}}_{\mathrm{C_\alpha X}} & \text{for } \mathbf{R}_{\mathrm{C_\alpha C_\beta}}\cdot\tilde{\mathbf{R}}_{\mathrm{C_\alpha X}} \le 0, \\ -\tilde{\mathbf{R}}_{\mathrm{C_\alpha X}} & \text{otherwise,} \end{cases} \tag{2}$$

where

$$\tilde{\mathbf{R}}_{\mathrm{C_\alpha X}} = \frac{1}{\sin\theta_{\mathrm{H_4C_\alpha H_5}}}\left(\frac{\mathbf{R}_{\mathrm{C_\alpha H_5}}}{|\mathbf{R}_{\mathrm{C_\alpha H_5}}|}\times\frac{\mathbf{R}_{\mathrm{C_\alpha H_4}}}{|\mathbf{R}_{\mathrm{C_\alpha H_4}}|}\right). \tag{3}$$

With these definitions, the dihedral and rocking angles, which we consider in this paper, are expressed as $\phi_{\mathrm{MuC_\beta C_\alpha X}}$ and $\theta_{\mathrm{C_\beta C_\alpha X'}}$, respectively.

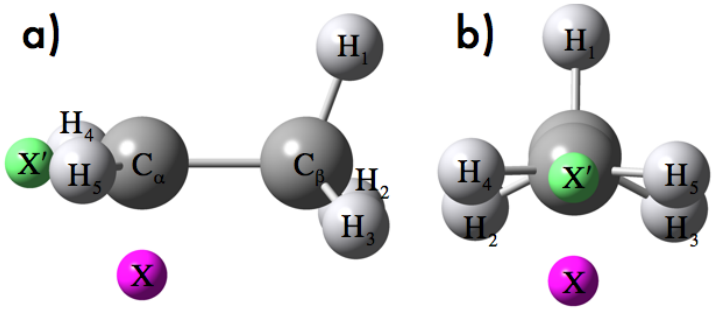

FIG. 1: a) Side and b) front views of the ethyl radical optimized by the PM6 method. The positions X$'$ and X, indicated by green and purple balls, respectively, are introduced to define the rocking and dihedral angles (See text for details). The H$_1$ atom was substituted with a Mu atom in the PIMD simulations.

The standard imaginary-time PIMD simulations in normal mode coordinates [12, 13] were performed to obtain thermal equilibrium structures including the nuclear quantum effect directly. The partition function for the canonical ensemble in the quantum statistics is represented as

$$Z(\beta) = \mathrm{Tr}\left[\exp\left(-\beta\hat{H}\right)\right], \tag{4}$$

in which $\beta = 1/k_{\mathrm{B}}T$ where k_{B} and T are the Boltzmann constant and temperature, respectively, and $\hat{H}$ is the Hamiltonian of the M quantum particle system. According to the PI scheme, Eq. (4) is rewritten as an $M\times P$ classical particle system:

$$Z(\beta) = \lim_{P\to\infty}\prod_{i=1}^{M}\left(\frac{m_i P}{2\pi\beta\hbar^2}\right)^{3P/2}\int d\mathbf{R}_i^{(1)}d\mathbf{R}_i^{(2)}\cdots d\mathbf{R}_i^{(s)}\cdots d\mathbf{R}_i^{(P)}\exp\left(-\beta V_{\mathrm{eff}}\right). \tag{5}$$

In this equation P and $\hbar$ are the number of the imaginary time slice and the reduced Plank constant, respectively; m_i and $\mathbf{R}_i^{(s)}$ are the mass of the ith nucleus and the coordinate of the sth slice of the ith nucleus, respectively; and V_{eff} is expressed as

$$V_{\text{eff}} = \sum_{s=1}^{P} \sum_{i=1}^{M} \left\{ \frac{m_i P}{2\beta^2\hbar^2} \left(\mathbf{R}_i^{(s+1)} - \mathbf{R}_i^{(s)} \right)^2 \right\} + \frac{1}{P} V \left(\mathbf{R}_1^{(s)}, \mathbf{R}_2^{(s)}, \cdots, \mathbf{R}_M^{(s)} \right). \tag{6}$$

In this paper, we used the Born-Oppenheimer potential energy values and their first derivatives with respect to the nuclei positions generated *on the fly* by the PM6 method. The PIMD simulations were conducted with our PIMD code [9], which is connected to an MOPAC 2012 package.

To effectively control the system temperature, the massive Nosé-Hoover chain thermostat with chain length parameter 4 was chosen for our PIMD simulation, where the equation of motion was integrated using the velocity-Verlet time integrator with the multiple time step technique [14]. The PIMD simulations were performed at 300 K using the various Trotter numbers (number of beads) of P = 16 – 512 with the imaginary-time increment dt = 40 asec. Each sampling run was conducted for 45,000 steps after a thermal equilibration of 5,000 steps, judging from the convergence in the temperature and the radius of gyration of the μ^+ cloud.

III. RESULTS AND DISCUSSION

III-1. Convergence of the number of beads for a muon

To determine the appropriate number of beads for the μ^+ cloud, some PIMD simulations were performed by changing the number of beads (P) from 16 to 512. Table I shows the convergence in average total energy, calculated through a virial estimator with the potential and first derivative terms obtained from the PM6 method, together with the convergence in the average C$_\beta$-Mu lengths ($R_{\text{C}_\beta\text{Mu}}$). These energies in the small number of beads are lower than the conventional PM6 energy with the zero-point energy (ZPE) correction. While it is essential to use 64 or more beads to represent well the contribution of the quantum and thermal effects, neither the energy nor bond length seems to change drastically when 64 beads are employed to describe the quantum particles. Thus, in the following discussion we show the PIMD results with P set to 64.

III-2. Structural parameters

In Table II, we summarize the average bond lengths $R_{\text{C}_\beta\text{Mu}}$, $R_{\text{C}_\beta\text{H}_\beta}$, $R_{\text{C}_\alpha\text{H}_\alpha}$, and $R_{\text{C}_\beta\text{C}_\alpha}$ and average bond angles $\theta_{\text{MuC}_\beta\text{C}_\alpha}$, $\theta_{\text{H}_\beta\text{C}_\beta\text{C}_\alpha}$, $\theta_{\text{C}_\beta\text{C}_\alpha\text{H}_\alpha}$, and $\theta_{\text{C}_\beta\text{C}_\alpha\text{X}'}$ by the PIMD simulations, together with the equilibrium (EQ) ones as well as the dihedral angle $\phi_{\text{MuC}_\beta\text{C}_\alpha\text{X}}$ by the conventional PM6 method. Here, $R_{\text{C}_\beta\text{H}_\beta}$, $R_{\text{C}_\alpha\text{H}_\alpha}$, $\theta_{\text{H}_\beta\text{C}_\beta\text{C}_\alpha}$, and $\theta_{\text{C}_\beta\text{C}_\alpha\text{H}_\alpha}$ are the averages of $R_{\text{C}_\beta\text{H}_2}$ and $R_{\text{C}_\beta\text{H}_3}$, $R_{\text{C}_\alpha\text{H}_4}$ and $R_{\text{C}_\alpha\text{H}_5}$, $\theta_{\text{H}_2\text{C}_\beta\text{C}_\alpha}$ and $\theta_{\text{H}_3\text{C}_\beta\text{C}_\alpha}$, and $\theta_{\text{C}_\beta\text{C}_\alpha\text{H}_4}$ and $\theta_{\text{C}_\beta\text{C}_\alpha\text{H}_5}$, respectively.

Table II clearly shows that all the average bond lengths obtained from the PIMD

TABLE I: Bead dependence in total energy and C_β-Mu length in the PIMD simulations.

Methods	Number of Beads (P)	Total Energy [kcal/mol]	$R_{C_\beta Mu}$ [Å]
PIMD[a]	16	−7154.59	1.133
	32	−7150.84	1.138
	64	−7148.89	1.144
	128	−7148.49	1.143
	256	−7149.08	1.141
	512	−7148.14	1.143
Conventional MO[b]	—	−7149.63	1.104

[a] Total energies and bond lengths are average values of those in each of 45,000 steps.
[b] Total energy is corrected using zero-point energy with a Mu atom.

TABLE II: Structural parameters of muoniated ethyl radical from the PIMD simulation (average values) and conventional PM6 calculation.

	PIMD	EQ
Bond Length [Å]		
$R_{C_\beta Mu}$	1.144	1.104
$R_{C_\beta H_\beta}$	1.114	1.099
$R_{C_\alpha H_\alpha}$	1.080	1.068
$R_{C_\beta C_\alpha}$	1.471	1.465
Bond Angle [degree]		
$\theta_{MuC_\beta C_\alpha}$	111.1	110.3
$\theta_{H_\beta C_\beta C_\alpha}$	112.1	112.5
$\theta_{C_\beta C_\alpha H_\alpha}$	120.7	121.0
$\theta_{C_\beta C_\alpha X'}$	168.0	179.4
Dihedral Angle [degree]		
$\phi_{MuC_\beta C_\alpha X}$	—	180.0

simulations are longer than those of the EQ ones. Especially, $R_{C_\beta Mu}$ is 1.144 Å, which is about 0.04 Å longer than the corresponding EQ one of 1.104 Å. The elongation of $R_{C_\beta Mu}$ occurs because the PIMD simulation can take account of the nuclear quantum and thermal effects under the anharmonicity of the potential. Note that such anharmonicity is ignored in the normal mode vibrational analysis with the harmonic approximation by conventional

QM calculations. In contrast, there are only slight differences in the bond angle between the structures. In the EQ structure the methylene group is likely to be described by an sp^2-hybridized C_α atom, as seen from $\theta_{C_\beta C_\alpha X'}$ in Table I, though this atom could plausibly be more sp^3 hybridized based on chemical intuition, due to electron repulsion between the CH_3 group and the unpaired electron.

In addition to the bond length, the nuclear quantum and thermal effects make a significant difference in the dihedral angles between the PIMD and EQ structures. To investigate the relation between these structural parameters, the two-dimensional (2D) distribution map as a function of $R_{C_\beta Mu}$ and $\phi_{MuC_\beta C_\alpha X}$ is shown in Fig. 2. It is noteworthy that while the structure with $\phi_{MuC_\beta C_\alpha X} = 0°$ is less stable than that with $\phi_{MuC_\beta C_\alpha X} = 180°$ (EQ structure), these structures have similar frequency in the PIMD simulations. This can be attributed to the *easy* inversion of the methylene group. $R_{C_\beta Mu}$ fluctuates around the average length (1.144 Å, denoted by the white broken line in Fig. 2) with amplitude of about 0.3 Å in the two restricted regions, to which the $C_\beta H_2Mu$-group rotation around C_β-C_α axis is confined. Accordingly, there is a characteristic correlation between $R_{C_\beta Mu}$ and $\phi_{MuC_\beta C_\alpha X}$. On the other hand, various experimental studies have revealed that the rotational barrier of the CH_2Mu group is much higher than that of the CH_3 group of the hydrogenated ethyl radical [15]; the former is about 0.7 kcal/mol comparable to the contribution of k_BT, and the latter is about 0.06 kcal/mol. Our PIMD simulation with the semiempirical PM6 method seems to provide such motion of the $C_\beta H_2Mu$-group rotation.

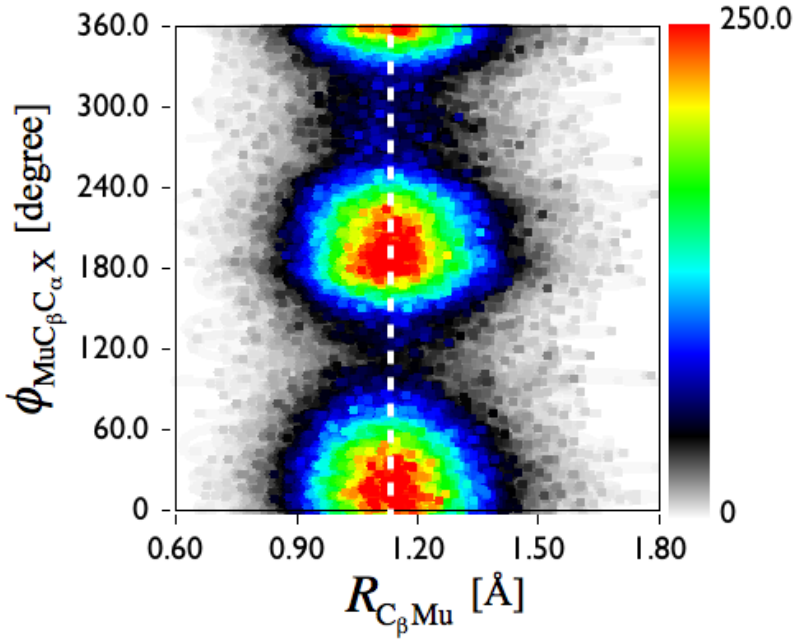

FIG. 2: Two-dimensional distribution of the bond length and dihedral angle.

We next focused on the rocking motion of the methylene group. Fig. 3 shows the 2D

distribution map of the dihedral angle $\phi_{\mathrm{MuC}_\beta\mathrm{C}_\alpha\mathrm{X}}$ and rocking angle $\theta_{\mathrm{C}_\beta\mathrm{C}_\alpha\mathrm{X}'}$, and demonstrates that the rocking motion is dependent on the dihedral angle. This motion is expected to be associated directly with the description of the radical orbital on the C_α atom, and thus indirectly with the $\mathrm{C}_\beta\mathrm{H}_2\mathrm{Mu}$-group motion. This idea is supported by the following two considerations: 1) the rocking angle changes in conjunction with the ratio between sp^2 and sp^3 hybridizations of the methylene C_α atom, which is critically involved in the shape of the radical orbital. 2) This orbital shape is influenced by the $\mathrm{C}_\beta\mathrm{H}_2\mathrm{Mu}$-group motion in light of the steric relation of the C_β-H and C_β-Mu bonding orbitals. In addition, as listed in Table II, $\theta_{\mathrm{C}_\beta\mathrm{C}_\alpha\mathrm{X}'}$ in the PIMD *average* structure is smaller than that in the EQ structure, indicating that the radical orbital has a tendency to be the sp^3-hybridized one. Therefore, the PIMD technique improves on the poor description of the unpaired electronic structure of the methylene group given by the semiempirical approximation.

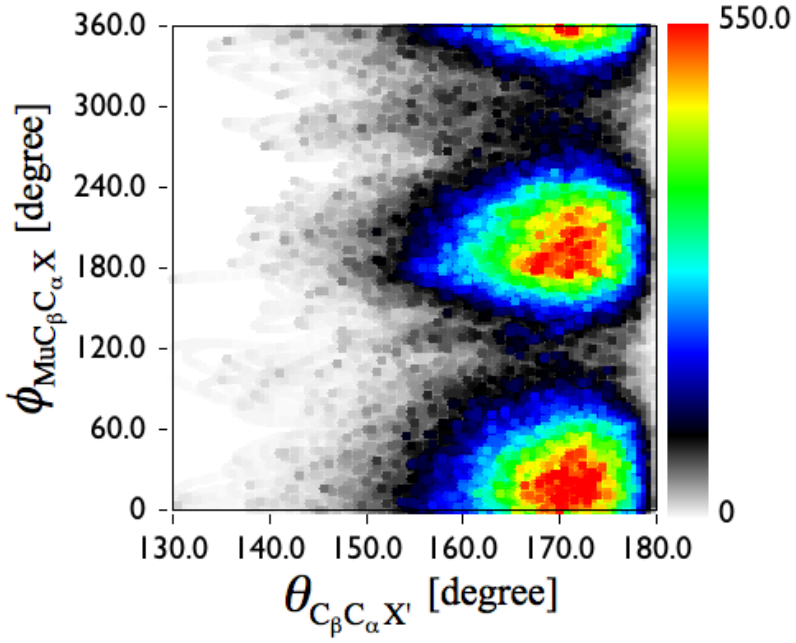

FIG. 3: Two-dimensional distribution of the rocking angle and dihedral angle.

III-3. Isotropic hyperfine coupling constant (HFCC)

Table III presents the isotropic hyperfine coupling constants (HFCCs) of the muon and proton in muoniated ethyl radical estimated by the PIMD simulation and conventional PM6 method, together with the corresponding experimental values in the gas phase at about 300 K [15]. The average values of the HFCCs obtained from the PM6 method over the PIMD simulation are listed in the PIMD column. A_μ and A_{p_β} denote the μ HFCC and the average proton HFCC of the H_2 and H_3 atoms, respectively. A'_μ is the reduced μ

HFCC in order to compare with the proton HFCC, represented by

$$A'_\mu = \frac{\mu_\mathrm{p}}{\mu_\mu} A_\mu. \tag{7}$$

$\bar{A}_\beta$ is the average of the HFCCs for the CH_2Mu group, defined as

$$\bar{A}_\beta = \frac{\left(A'_\mu + 2A_{\mathrm{p}_\beta}\right)}{3}, \tag{8}$$

and A_{p_α} indicates the average of the proton HFCCs of the H_4 and H_5 atoms.

TABLE III: Isotropic hyperfine coupling constants of the muon and proton in muoniated ethyl radical, which are obtained from the PIMD simulation (300 K), conventional PM6 calculation (0 K), and experiment in the gas phase (about 300 K)[a] [mT].

	PIMD	EQ	Exptl.
A_μ	27.0	(6.7)	11.8
A'_μ	8.5	2.1	3.70
A_{p_β}	10.9	14.3	2.38
$\bar{A}_\beta$	10.1	10.2	2.82
A_{p_α}	7.6	8.9	−2.26

[a] The values are drawn from Table II of Ref. [16].

We found a noticeable change in the HFCC attributable to the nuclear quantum and thermal effects, though much larger values and opposite-sign value (A_{p_α}) are provided compared to the experimental values. The significant A_μ and A_{p_β} are responsible for the spin polarization of α electrons at the Mu and H_β atoms as a result of that of the β electrons at the C_β atom, as seen in Table IV. The shortcoming of the PM6 method, such as less flexibility of the basis functions and less accuracy of 2-electron integrals, would cause overpolarization at the C_β atom to be orthogonalized with the unpaired α electron on the C_α atom. Inclusion of the nuclear quantum effect remedies the relation between A'_μ and A_{p_β} to be closer to the experimental one. Further, $\bar{A}_\beta$ and A_{p_α} are smaller than those in the EQ structure because of the CH_2Mu-group rotation. The significantly elongated $R_{\mathrm{C}_\beta\mathrm{Mu}}$ enhances the spin polarization of the β electron at the C_β atom, resulting in that only μ HFCC by the PIMD simulation is larger than the corresponding EQ value. Fig. 4 shows the 2D distribution map of the bond length and reduced μ HFCC, demonstrating that the μ HFCC tends to be larger as $R_{\mathrm{C}_\beta\mathrm{Mu}}$ is elongated. Fig. 5 gives the 2D distribution map of the dihedral angle and reduced μ HFCC; this illustrates that the μ HFCC would approach the experimental one, given that the structures with $\phi_{\mathrm{MuC}_\beta\mathrm{C}_\alpha\mathrm{X}} = 0°$ and/or 180° are more frequent. Although the sign of the spin population of the H_α atoms is opposite to that of the C_α atom, the proton HFCCs of these have positive signs, which are different from those of the experimental HFCCs. Further, the large HFCCs suggest that the distances

between an electron on the Mu or H atoms and an unpaired electron on the C_α atom become closer than expected. Thus the PIMD simulation using the PM6 method does not provide quantitative HFCC values.

TABLE IV: Atomic orbital spin populations in the equilibrium structure of the ethyl radical.

	Atom	Spin Population
C_β	2s	−0.00754
	2px	−0.00596
	2py	−0.03279
	2pz	−0.00541
H_1^a	1s	0.03943
H_β	1s	0.01106
C_α	2s	0.02532
	2px	0.95268
	2py	0.04116
	2pz	0.03948
H_α	1s	−0.03425

[a] substituted with a Mu atom in the PIMD simulation

The PM6 method cannot quantitatively describe the geometric and electronic structures involved with a radical orbital and then the muon and proton HFCCs, because such a radical orbital is difficult to treat under the semiempirical approximation. On the other hand, it is expected that the description of the CH_2Mu group, remotely relative to the radical orbital, would be valid rather than poor, because this group is composed of three covalent bonds. The time-consuming PIMD simulations with 64 beads using the density functional theory (DFT) method are now in progress; this method can provide a more accurate and reliable potential for muoniated/hydrogenated ethyl radicals.

IV. CONCLUDING REMARKS

We have performed *on-the-fly* PIMD simulations for muoniated ethyl radical using the semiempirical PM6 method with various numbers of beads (P = 16–512). It turned out that at least 64 beads are necessary to represent the μ^+ cloud. We have succeeded in describing the nuclear quantum effect on the muoniated ethyl radical. The bond lengths, e.g., $R_{C_\beta Mu}$, from our PIMD simulation are longer than those from the conventional PM6 method, in a reflection of the consideration of the nuclear quantum effect under the anharmonicity of the potential. In line with our expectations, the CH_2Mu-group rotational motion is correlated

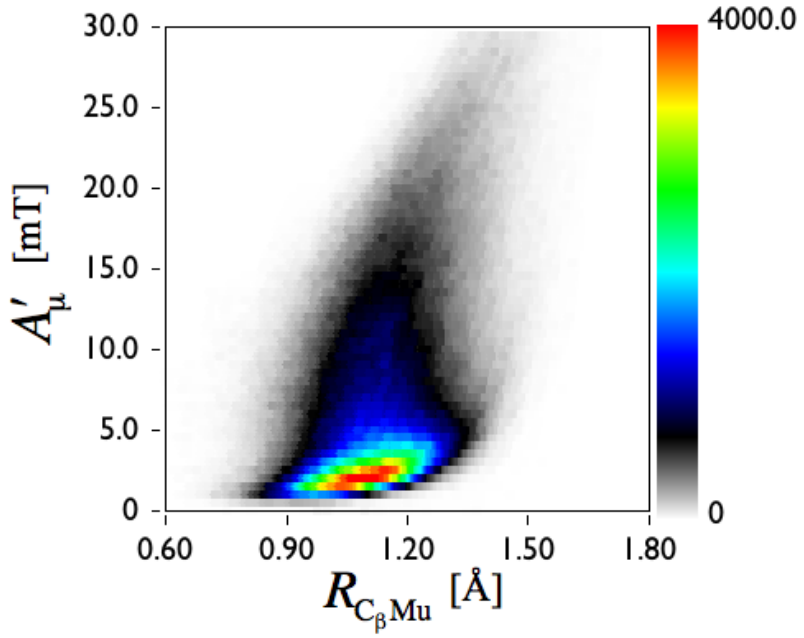

FIG. 4: Two-dimensional distribution of the bond length and reduced μ HFCC.

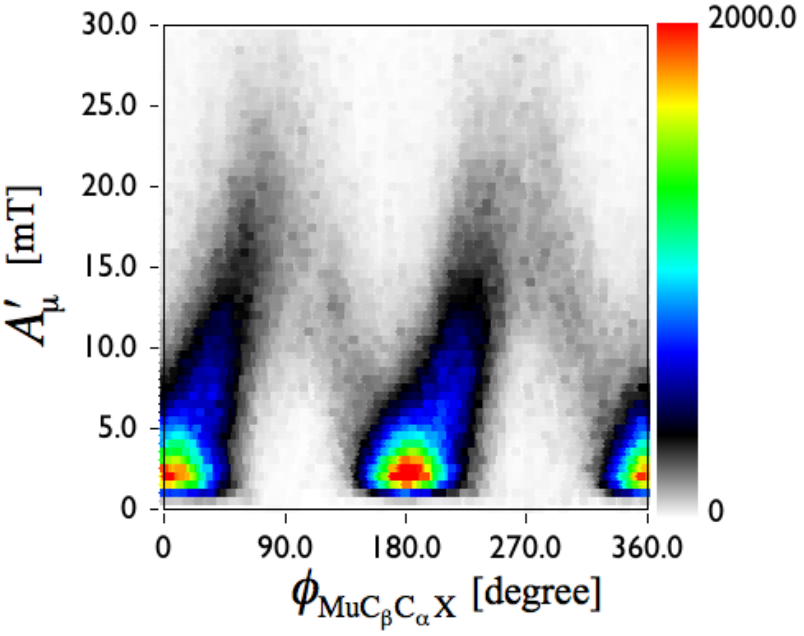

FIG. 5: Two-dimensional distribution of the dihedral angle and reduced μ HFCC.

with the C_β-Mu stretching motion and also the rocking motion of the methylene group. Inclusion of the nuclear quantum effect causes a drastic change in the muon and proton HFCCs. The values obtained from our simulation overestimate the experimental values because of the limitation of the semiempirical approach. It can be concluded that although the semiempirical PM6 method is less applicable to doublet systems, especially moieties with an unpaired electron, the $C_\beta H_2$Mu-group motion and large $R_{C_\beta Mu}$, arising from the nuclear quantum and thermal effects, make a substantial difference in the HFCC between the PIMD and conventional calculations.

Acknowledgements

The present study was supported by the Grand-in-Aid for Scientific Research by the Ministry of Education, Culture, Sports, Science, and Technology, Japan (Kakenhi). KY would like to thank the Yokohama Academic Foundation for its support of our project.

References

[1] C. J. Rhodes, J. Chem. Soc. Perkin Trans. **2**, 1379 (2002). doi: 10.1039/b100699l

[2] S. S. Gerstein and L. P. Ponomarev, Phys. Lett. B **72**, 80 (1977) doi: 10.1016/0370-2693(77)90067-3; Y. V. Petrov, Nature **285**, 466 (1980) doi: 10.1038/285466a0; S. E. Jones *et al.*, Phys. Rev. Lett. **51**, 1757 (1983); S. E. Jones, Nature **321**, 127 (1986); W. H. Breunlich, P. Kammel, J. S. Cohen, and M. Leon, Annu. Rev. Nucl. Part. Sci. **39**, 311 (1989). doi: 10.1146/annurev.ns.39.120189.001523

[3] D. G. Freming, S. P. Cottrell, I. McKenzie, and R. M. Macrae, Phys. Chem. Chem. Phys. **14**, 10953 (2012).

[4] T. Takayanagi, Chem. Phys. **334**, 109 (2007). doi: 10.1016/j.chemphys.2007.02.017

[5] S. F. J. Cox, Solid State NMR **11**, 103 (1998) doi: 10.1016/S0926-2040(97)00100-8; E. Roduner and H. Fischer, Chem. Phys. **54**, 261 (1981) doi: 10.1016/0301-0104(81)80241-8; C. J. Rhodes, Annu. Rep. Prog. Chem., Sect. C: Phys. Chem. **97**, 315 (2001); R. West and P. W. Percival, Dalton Trans. **39**, 9209 (2010).

[6] V. Barone, in *Recent Advances in Density Functional Methods*, Part I, Ed. D. P. Chong (World Scientific Publ. Co., Singapore, 1996); S. A. Perera, J. D. Watts, and R. J. Bartlett, J. Chem. Phys. **100**, 1425 (1994) doi: 10.1063/1.466620; H. Sekino and R. J. Bartlett, J. Chem. Phys. **82**, 4225 (1985) doi: 10.1063/1.448837; C. J. Cramer and D. G. Truhlar, Phys. Chem. Chem. Phys. **11**, 10757 (2009).

[7] R. Improta and V. Barone, Chem. Rev. **104**, 1231 (2004) doi: 10.1021/cr960085f; L. Hermosilla, P. Calle, J. M. García de la Vega, and C. Sieiro, J. Phys. Chem. A **109**, 1114 (2005) doi: 10.1021/jp0466901; F. Neese, Coord. Chem. Rev. **253**, 526 (2009). doi: 10.1021/jp0466901

[8] M. Mella and D. C. Clary, J. Chem. Phys. **119**, 10048 (2003); T. Ishimoto, M. Tachikawa, and U. Nagashima, Int. J. Quant. Chem. **109**, 2677 (2009).

[9] K. Suzuki, M. Shiga, and M. Tachikawa, J. Chem. Phys. **129**, 144310-1 (2008).

[10] J. J. P. Stewart, J. Mol. Model. **13**, 1173 (2007). doi: 10.1007/s00894-007-0233-4

[11] MOPAC2012, James J. P. Stewart, Stewart Computational Chemistry, Colorado Springs, CO, USA, HTTP://OpenMOPAC.net (2012).

[12] D. Marx and M. Parrinello, Z. Phys. B **95**, 143 (1994).
[13] B. J. Berne and D. Thirumalai, Ann. Rev. Phys. Chem. **37**, 401 (1986). doi: 10.1146/annurev.pc.37.100186.002153
[14] G. J. Martyna, M. L. Klein, and M. Tuckerman, J. Chem. Phys. **97**, 2635 (1992). doi: 10.1063/1.463940
[15] B. Webster and D. Buttar, J. Chem. Soc., Faraday Trans. **92**, 2331 (1996). doi: 10.1039/ft9969202331
[16] P. W. Percival *et al.*, Chem. Phys. Lett. **163**, 241 (1989). doi: 10.1016/0009-2614(89)80043-0